Power-Efficient and Cost-Effective 2-D Symmetry Filter Architectures

Pei-Yu Chen, *Student Member, IEEE*, Lan-Da Van, *Member, IEEE*, I-Hung Khoo, *Member, IEEE*, Hari C. Reddy, *Fellow, IEEE*, and Chin-Teng Lin, *Fellow, IEEE*

***Abstract*—This paper presents two-dimensional (2-D) VLSI digital filter structures possessing various symmetries in the filter magnitude response. For this purpose, four Type-1 and four Type-2 power-efficient and cost-effective 2-D magnitude symmetry filter architectures possessing diagonal, fourfold rotational, quadrantal, and octagonal symmetries with reduced number of multipliers and one power-efficient and cost-effective multimode 2-D symmetry filter are given. By combining the identities of the four Type-1 symmetry filter structures, the proposed multimode 2-D symmetry filter is capable of providing four different operation modes: diagonal symmetry mode (DSM), fourfold rotational symmetry mode (FRSM), quadrantal symmetry mode (QSM), and octagonal symmetry mode (OSM). The proposed diagonal, fourfold rotational, quadrantal, and octagonal symmetry filter structures can attain power savings of 16.77%, 36.30%, 22.90%, and 37.73% with respect to that of the conventional 2-D filter design without symmetry. On the other hand, the proposed DSM, FRSM, QSM, and OSM modes can reduce power consumption by 11.01%, 31.42%, 17.53%, and 35.26% compared with that of the conventional 2-D filter design. The proposed multimode filter can result in a 63.25% area reduction compared with the sum of the areas of the four individual Type-1 symmetry filter structures.**

***Index Terms*—Cost effective, multimode, power efficient, symmetry filter, 2-D filter.**

I. Introduction

TWO-DIMENSIONAL (2-D) digital filters are widely used in a variety of digital signal processing (DSP) systems such as image restoration [1], [2], image enhancement [3], frequency response analysis [4]–[7], and beamformer [8], [9]. Although 2-D digital filters can be simulated on a general purpose computer for the above applications, dedicated computing structures are needed in order to meet the high throughput demands. Several conventional very large scale integration (VLSI) architectures for 2-D filters have been studied in [10]–[12], and an existing application-specific integrated circuit (ASIC) approach has been applied to the design of beam filter [8], [9], 2-D diagonal symmetry filter [13], [14], and fourfold rotational symmetry filter [15]. Recently the authors have presented 2-D digital filter architectures with separable denominators [13]. The significant feature of filters studied in [13] is that they exhibit the denominator separability as a filter structural property. This means that the separability of the denominator is maintained independent of the choice of multiplier values. This important property is essential for the design of the multimode symmetry filter discussed in this paper. In addition, the denominator separability is a requirement for the stability of quarter-plane 2-D transfer functions possessing quadrantal, fourfold rotational, and octagonal magnitude symmetries. Further, the filter architectures in [13] are shown to realize the filters possessing diagonal symmetry and separable denominators with fewer multipliers than other architectures presented in [14] and [15]. Thus, all the above indicates that the separable structures in [13] are highly suitable for the design of 2-D filters possessing various magnitude symmetries.

It is well-known that symmetry presented in the frequency responses of 2-D filters can be used to reduce the number of multipliers [5]–[7]; however, the corresponding 2-D filter architectures have not been fully explored. In this paper, eight power- efficient and cost-effective symmetry filter architectures based on the structures in [13] are presented (four Type-1 and four Type-2). They possess diagonal, fourfold rotational, quadrantal, and octagonal symmetries, and require less number of multipliers. Further, in order to integrate the support of multiple symmetry functions, one power-efficient and cost-effective Type-1 multimode 2-D filter design with four symmetries is proposed. The new multimode structure providing four modes can attain power reduction by 11.01%, 31.42%, 17.53%, and 35.26% compared with that of the conventional 2-D filter design without symmetry [12].

This paper is organized as follows. Section II briefly reviews the separable denominator filter transfer function and proposes the corresponding Type-1 and Type-2 structures. In Section III, four Type-1 and four Type-2 cost-effective symmetry filter structures with less number of multipliers are presented. The generalized design procedure of the Type-1 and Type-2 symmetry filters is addressed. A cost-effective Type-1 multimode filter architecture with four symmetries is discussed in Section IV. The power consumption and core area of the proposed symmetry filter structures and the multimode filter architecture are profiled and evaluated in Section V. Finally, the conclusions are given in Section VI.

II. Preliminaries of Separable Denominator Filter

The general transfer function of a 2-D IIR quarter-plane digital filter can be represented as

$$H(z_1,z_2)=\frac{Y(z_1,z_2)}{X(z_1,z_2)}=\frac{\sum_{i=0}^{N_1}\sum_{j=0}^{N_2}a_{ij}z_1^{-i}z_2^{-j}}{\sum_{i=0}^{N_1}\sum_{j=0}^{N_2}b_{ij}z_1^{-i}z_2^{-j}} \quad (1)$$

where $X(z_1,z_2)$ and $Y(z_1,z_2)$ denote the input and output of the digital filter, respectively, a_{ij} and b_{ij} denote the numerator and denominator coefficients, respectively, and $b_{00}=1$, $N_1\times N_2$ is the order of the IIR digital filter. Throughout this paper, we

Manuscript received January 22, 2010; revised May 05, 2010; accepted June 10, 2010. Date of current version December 30, 2010. The partial and related work of this paper was presented at 2008 APCCAS and 2009 ISCAS. This work was supported in part by the National Science Council Grant NSC-98-2220-E-009-042 and NSC-97-2220-E-009-024. This paper was recommended by Associate Editor J. S. Chang.

P. Y. Chen, L. D. Van, H.C. Reddy, and C. T. Lin are with the Department of Computer Science, National Chiao Tung University, Hsinchu, 300 Taiwan (e-mail: ldvan@cs.nctu.edu.tw)

I. H. Khoo and H. C. Reddy are with the Department of Electrical Engineering, California State University Long Beach, Long Beach, CA 90840 USA.

Color versions of one or more of the figures in this paper are available online at http://ieeexplore.ieee.org.

Digital Object Identifier 10.1109/TCSI.2010.2055274

assume that an image $M_1 \times M_2$ is fed to the following structures in raster-scan mode, and thus the delay $z_2^{-1} = z^{-1}$ and $z_1^{-1} = z^{-M_2}$, where z^{-1} and M_2 denote a unit delay element and the width of an image, respectively. A separable denominator transfer function is adopted in this paper due to the following reasons. First, the separable denominator is needed in realizing stable 2-D magnitude responses possessing various symmetries [5]–[7] of quarter-plane filters with the exception of diagonal symmetry. Second, the stability of this transfer function is easy to detect by simply calculating the poles of the two one-dimensional (1-D) polynomials. Third, the transfer function with symmetry requires fewer multipliers to realize [5]–[7]. Consider the separable denominator transfer function described in (2)

$$H(z_1,z_2) = \frac{Y(z_1,z_2)}{X(z_1,z_2)} = \frac{\sum_{i=0}^{N_1}\sum_{j=0}^{N_2} a_{ij} z_1^{-i} z_2^{-j}}{\left(1-\sum_{i=1}^{N_1} b_{i0} z_1^{-i}\right)\cdot\left(1-\sum_{j=1}^{N_2} b_{0j} z_2^{-j}\right)}. \quad (2)$$

Without loss of generality, we can assume the filter order $N_1 = N_2 = N$. Since the fourfold rotational and octagonal symmetry filter structures are the same when $N = 2, N = 3$ is selected in the following proposed filter structures. The Type-1 separable denominator transfer function of the 2-D filter can be recast in (3)

$$H(z_1,z_2) = \frac{Y_1(z_1,z_2)}{X(z_1,z_2)} \cdot \frac{Y(z_1,z_2)}{Y_1(z_1,z_2)} \quad (3)$$

where $Y_1(z_1,z_2)/X(z_1,z_2)$ is defined in (4)

$$Y_1 = X + \sum_{i=1}^{N} b_{i0} z_1^{-i} Y_1 \quad (4)$$

where $X = X(z_1,z_2)$ and $Y_1 = Y_1(z_1,z_2)$. Thus, $Y(z_1,z_2)/Y_1(z_1,z_2)$ can be generally represented as follows:

$$Y = \sum_{i=0}^{N}\sum_{j=0}^{N} a_{ij} z_1^{-i} z_2^{-j} Y_1 + \sum_{j=1}^{N} b_{0j} z_2^{-j} Y \quad (5)$$

where $Y = Y(z_1,z_2)$. The proposed Type-1 3×3 2-D IIR filter with separable denominator is depicted in Fig. 1 [13]. It can be verified through Mason's Gain Formula [16] that the structures of Block 1 and Block 2 in Fig. 1 satisfy (4) and (5), respectively, with $N = 3$ (It is to be noted that to verify (5), one needs to always treat X as the input and to determine Y/X and Y_1/X. That gives the relationship between Y and Y_1. This is true for all the structures discussed in this paper). Since the image is raster scanned, the delay $z_1^{-1} = z^{-M_2}$ is realized by a shift-register (SR) with size of M_2.

Similarly, the Type-2 separable denominator transfer function of the 2-D filter can again be recast in (6) as

$$H(z_1,z_2) = \frac{Y_2(z_1,z_2)}{X(z_1,z_2)} \cdot \frac{Y(z_1,z_2)}{Y_2(z_1,z_2)} \quad (6)$$

where $Y_2(z_1,z_2)/X(z_1,z_2)$ is defined in (7)

$$Y_2 = X + \sum_{j=1}^{N} b_{0j} z_2^{-j} Y_2 \quad (7)$$

where $Y_2 = Y_2(z_1,z_2)$. Thus, $Y(z_1,z_2)/Y_2(z_1,z_2)$ can be generally represented as follows:

$$Y = \sum_{i=0}^{N}\sum_{j=0}^{N} a_{ij} z_1^{-i} z_2^{-j} Y_2 + \sum_{i=1}^{N} b_{i0} z_1^{-i} Y. \quad (8)$$

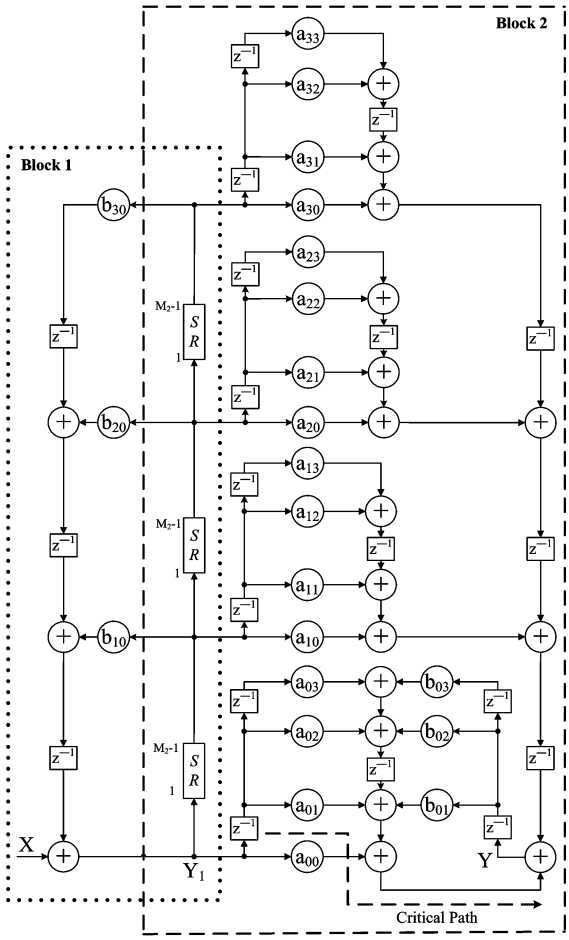

Fig. 1. Proposed Type-1 separable denominator 2-D IIR filter structure for $N = 3$ [13].

The proposed Type-2 3×3 2-D IIR filter with separable denominator is shown in Fig. 2[13]. The structures of Block 3 and Block 4 in Fig. 2 satisfy (7) and (8), respectively, with $N = 3$. The reason for writing the transfer function in (2) in the form of (3) followed by (4) and (5) as well as (6) followed by (7) and (8) is to decompose the filter structure into the two blocks in Figs. 1 and 2. Also, note that the structure in Fig. 2 is obtained by taking the transpose of the structure in Fig. 1. Using the tree method mentioned in [12] to arrange the adders, the critical periods in Figs. 1 and 2 are analyzed as $T_m + 3T_a$ and $T_m + 2T_a$, respectively, where T_m and T_a denote the operation time required by the multiplier and adder, respectively.

III. Cost-Effective 2-D Filter Architectures With Specific Symmetry

The presence of symmetry in the 2-D frequency response can alleviate the design complexity of a 2-D digital filter. Symmetry in the frequency response induces certain relationship among the filter coefficients which can result in fewer multipliers in the implementation. In this section, we will design eight symmetry filter architectures with diagonal, fourfold rotational, quadrantal and octagonal symmetry property.

A. Diagonal Symmetry Filter Structure

A 2-D magnitude response possesses diagonal symmetry if $|H(z_1,z_2)| = |H(z_2,z_1)|$ with $z_1 = e^{j\theta_1}$ and $z_2 = e^{j\theta_2}$, $\forall\,(\theta_1,\theta_2)$ [5]–[7]. Assuming the separable denominator transfer function in (2) is adopted, it will have diagonal symmetry if

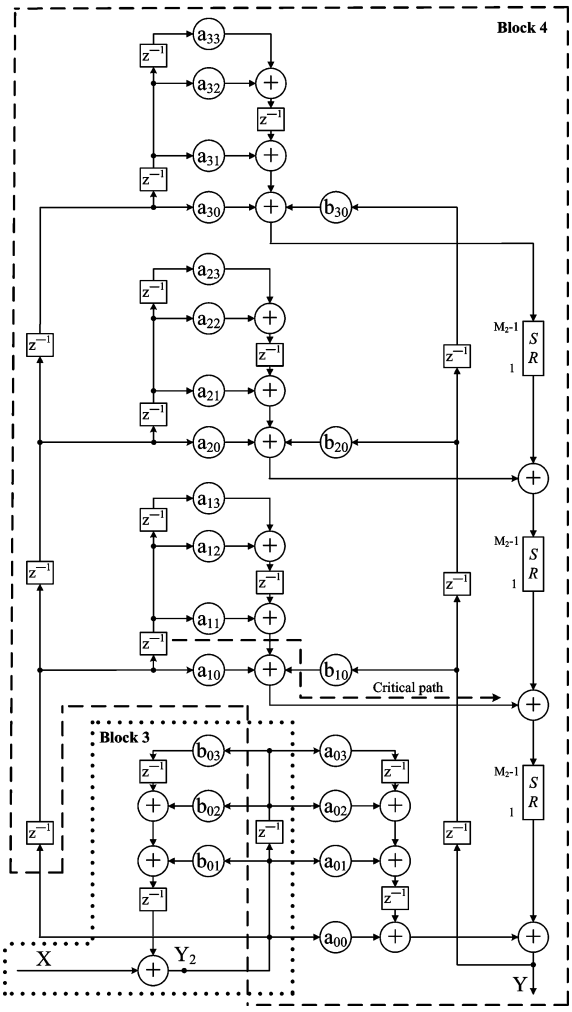

Fig. 2. Proposed Type-2 separable denominator 2-D IIR filter structure for $N = 3$ [13].

$a_{ij} = a_{ji}$ and $b_{k0} = b_{0k}$ for all i, j, k. Applying these constraints to the transfer function in (2), (4) and (5) can be recast in (9a) and (9b), respectively

$$Y_1 = X + \sum_{j=1}^{N} b_{0j} z_1^{-j} Y_1 \tag{9a}$$

$$Y = \sum_{j=1}^{N} b_{0j} z_2^{-j} Y + \sum_{i=0}^{N} a_{ii} z_1^{-i} z_2^{-i} Y_1 + \sum_{i=0}^{N-1} \sum_{j=i+1}^{N} a_{ij} \left(z_1^{-i} z_2^{-j} + z_1^{-j} z_2^{-i} \right) Y_1 \tag{9b}$$

and (7) and (8) can be recast in (10a) and (10b), respectively

$$Y_2 = X + \sum_{j=1}^{N} b_{0j} z_2^{-j} Y_2 \tag{10a}$$

$$Y = \sum_{j=1}^{N} b_{0j} z_1^{-j} Y + \sum_{i=0}^{N} a_{ii} z_1^{-i} z_2^{-i} Y_2 + \sum_{i=0}^{N-1} \sum_{j=i+1}^{N} a_{ij} \left(z_1^{-i} z_2^{-j} + z_1^{-j} z_2^{-i} \right) Y_2. \tag{10b}$$

According to (9a) and (9b) with $N = 3$, the Type-1 2-D diagonal symmetry filter structure with separable denominator is obtained and shown in Fig. 3. It can be shown that the structure satisfies (9a) as well as (9b) with $N = 3$. Similarly, in accordance with (10a) and (10b) with $N = 3$, the Type-2 2-D diagonal symmetry filter structure with separable denominator is obtained in Fig. 4. This structure satisfies (10a) as well as (10b) with $N = 3$. Using the tree method to arrange the adders, the critical paths are analyzed as $T_m + 3T_a$ and $T_m + 2T_a$ as shown in Figs. 3 and 4, respectively.

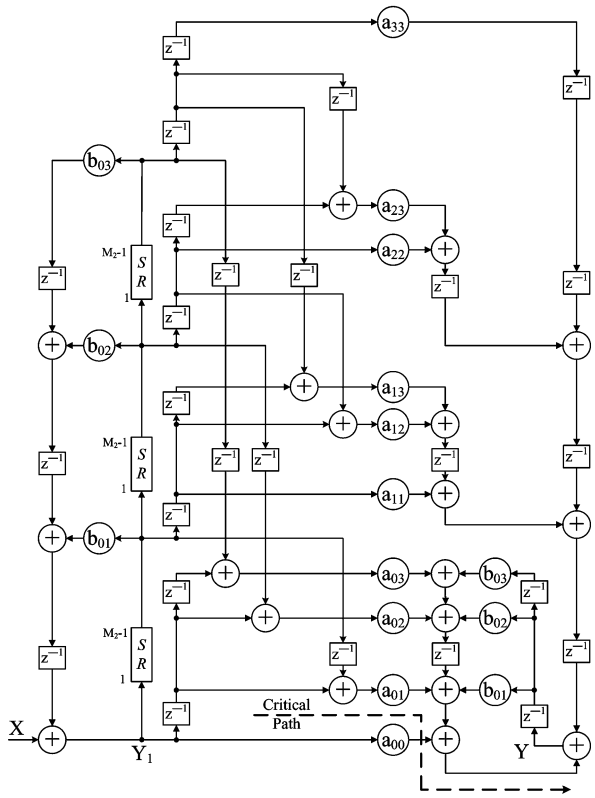

Fig. 3. Proposed Type-1 2-D diagonal symmetry filter structure with separable denominator for $N = 3$.

B. Fourfold Rotational Symmetry Filter Structure

For a 2-D magnitude response, if $|H(z_1, z_2)| = |H(z_2^{-1}, z_1)|$ with $z_1 = e^{j\theta_1}$ and $z_2 = e^{j\theta_2}$, $\forall\ (\theta_1, \theta_2)$, the filter possesses fourfold rotational symmetry [5]–[7]. With the separable denominator transfer function in (2), the following constraints on the coefficients will provide the required symmetry: $a_{ij} = a_{j(N-i)}$ and $b_{k0} = b_{0k}$ for all i, j, k. Applying these constraints to the transfer function in (2), (4) and (5) can be recast in (11a) and (11b), respectively

$$Y_1 = X + \sum_{j=1}^{N} b_{0j} z_1^{-j} Y_1 \tag{11a}$$

$$Y = \sum_{j=1}^{N} b_{0j} z_2^{-j} Y + v a_{uu} z_1^{-u} z_2^{-u} Y_1 + \sum_{i=0}^{u-v} \sum_{j=i}^{N-i-1} a_{ij} \times \left(z_1^{-i} z_2^{-j} + z_1^{-j} z_2^{-(N-i)} + z_1^{-(N-i)} z_2^{-(N-j)} + z_1^{-(N-j)} z_2^{-i} \right) Y_1 \tag{11b}$$

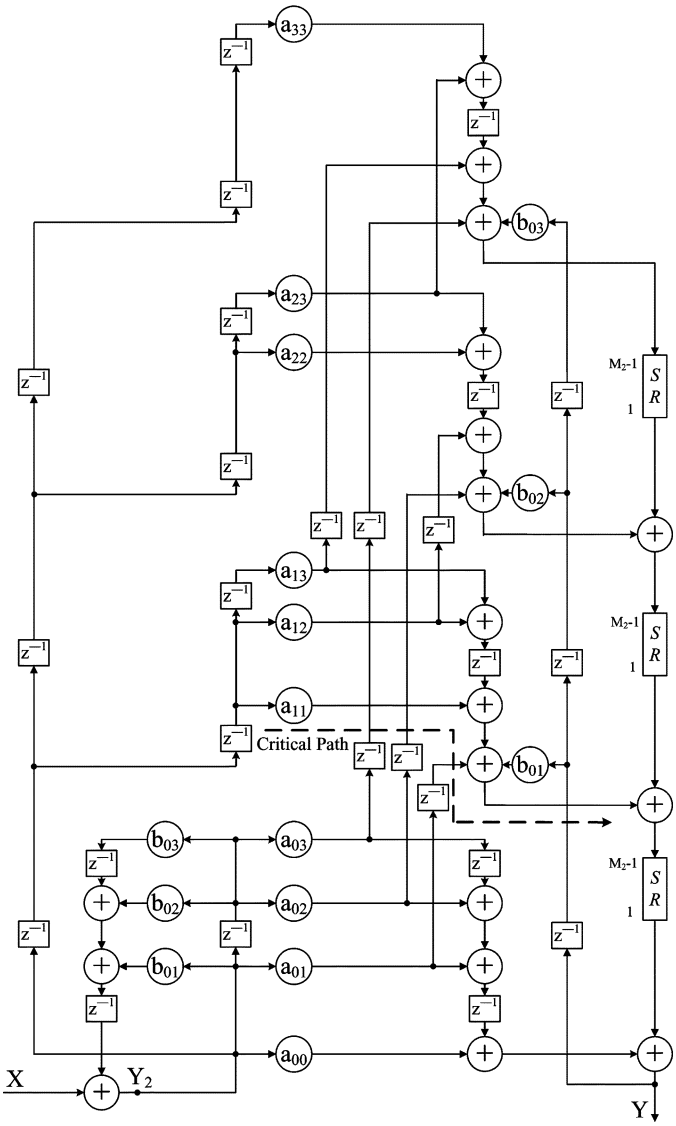

Fig. 4. Proposed Type-2 2-D diagonal symmetry filter structure with separable denominator for $N = 3$ [13].

and (7) and (8) can be recast in (12a) and (12b), respectively

$$Y_2 = X + \sum_{j=1}^{N} b_{0j} z_2^{-j} Y_2 \tag{12a}$$

$$\begin{aligned} Y = {} & \sum_{j=1}^{N} b_{0j} z_1^{-j} Y + v a_{uu} z_1^{-u} z_2^{-u} Y_2 \\ & + \sum_{i=0}^{u-v} \sum_{j=i}^{N-i-1} a_{ij} \\ & \times \left(z_1^{-i} z_2^{-j} + z_1^{-j} z_2^{-(N-i)} \right. \\ & \left. + z_1^{-(N-i)} z_2^{-(N-j)} + z_1^{-(N-j)} z_2^{-i} \right) Y_2 \end{aligned} \tag{12b}$$

where $u = \lfloor N/2 \rfloor$ and $v = (N+1)$ *mod 2*. Note that $\lfloor \bullet \rfloor$ denotes the largest integer that is smaller than or equal to $\bullet$. In the case of $N = 3$, (11a)-(11b) and (12a)-(12b) can be realized by Type-1 and Type-2 2-D fourfold rotational symmetry filter structures with separable denominator given in Figs. 5 and 6,

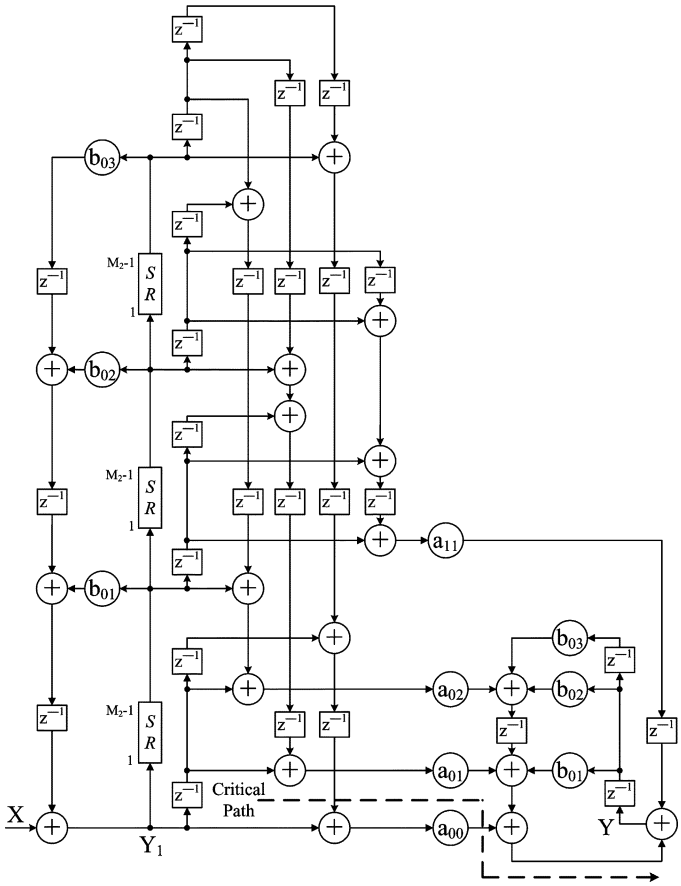

Fig. 5. Proposed Type-1 2-D fourfold rotational symmetry filter structure with separable denominator for $N = 3$.

respectively. It is easy to verify that the structure in Fig. 5 satisfies (11a) and (11b) with $N = 3$, and the filter structure in Fig. 6 satisfies (12a) and (12b). Using the tree method to arrange the adders, the critical paths are analyzed as $T_m + 3T_a$ and $T_m + 2T_a$ as shown in Figs. 5 and 6, respectively.

C. Quadrantal Symmetry Filter Structure

A 2-D magnitude response possesses quadrantal symmetry if $|H(z_1, z_2)| = |H(z_1^{-1}, z_2)|$ with $z_1 = e^{j\theta_1}$ and $z_2 = e^{j\theta_2}$, $\forall\, (\theta_1, \theta_2)$ [5]–[7]. Assuming the separable denominator transfer function in (2) is adopted, it will have quadrantal symmetry if $a_{ij} = a_{(N-i)j}$ and $b_{k0} = b_{0k}$ for all i, j, k. (Note that for quadrantal symmetry, b_{k0} need not be the same as b_{0k}; but here they are assumed equal to ease the implementation of the multimode filter to be discussed later). Applying the constraints to the transfer function in (2), (4) and (5) can be recast in (13a) and (13b), respectively

$$Y_1 = X + \sum_{j=1}^{N} b_{0j} z_1^{-j} Y_1 \tag{13a}$$

$$\begin{aligned} Y = {} & \sum_{j=1}^{N} b_{0j} z_2^{-j} Y + v \cdot \sum_{j=0}^{N} a_{uj} \left(z_1^{-u} z_2^{-j} \right) Y_1 \\ & + \sum_{i=0}^{u-v} \sum_{j=0}^{N} a_{ij} \left(z_1^{-i} z_2^{-j} + z_1^{-(N-i)} z_2^{-j} \right) Y_1 \end{aligned} \tag{13b}$$

and (7) and (8) can be recast in (14a) and (14b), respectively

$$Y_2 = X + \sum_{j=1}^{N} b_{0j} z_2^{-j} Y_2 \tag{14a}$$

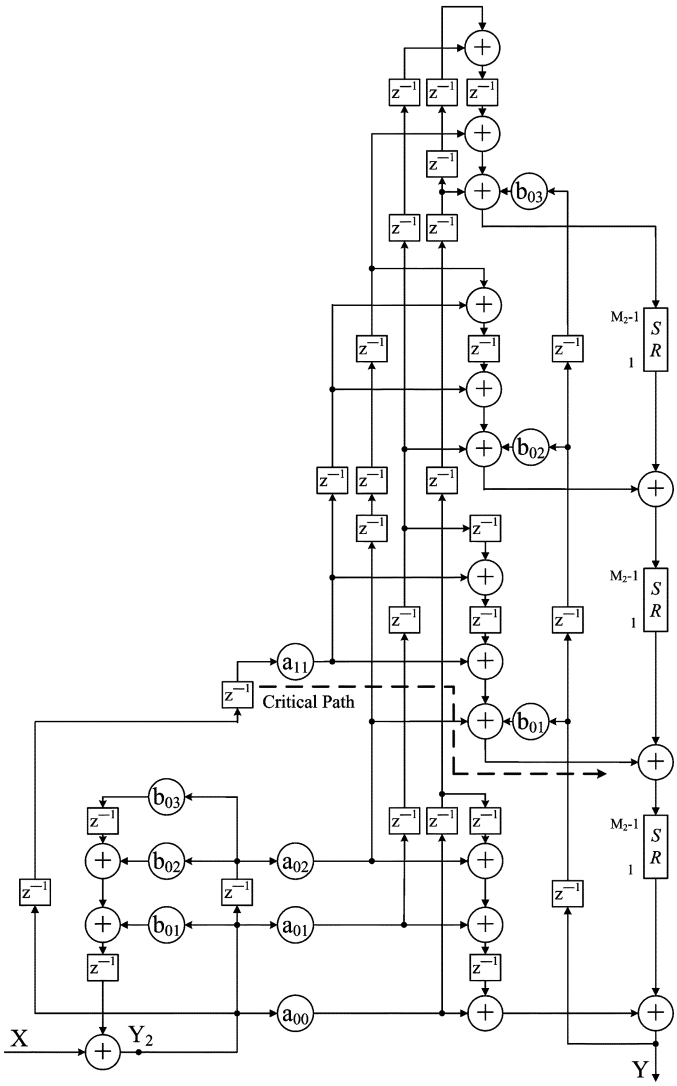

Fig. 6. Proposed Type-2 2-D fourfold rotational symmetry filter structure with separable denominator for $N = 3$.

$$Y = \sum_{j=1}^{N} b_{0j} z_1^{-j} Y + v \cdot \sum_{j=0}^{N} a_{uj} \left(z_1^{-u} z_2^{-j} \right) Y_2 + \sum_{i=0}^{u-v} \sum_{j=0}^{N} a_{ij} \left(z_1^{-i} z_2^{-j} + z_1^{-(N-i)} z_2^{-j} \right) Y_2. \quad (14b)$$

Taking into consideration (13a) and (13b) with $N = 3$, the Type-1 2-D quadrantal symmetry filter structure with separable denominator is realized as shown in Fig. 7. Similarly, in accordance with (14a) and (14b) with $N = 3$, the Type-2 2-D quadrantal symmetry filter structure with separable denominator is obtained in Fig. 8. Both architectures can be verified by Mason's Gain Formula. Using the tree method again to arrange the adders, the critical paths are analyzed as $T_m + 3T_a$ and $T_m + 2T_a$ as shown in Figs. 7 and 8, respectively.

D. Octagonal Symmetry Filter Structure

Octagonal symmetry is a combination of diagonal, fourfold rotational and quadrantal symmetries. Any two of the three symmetries are sufficient to guarantee that a 2-D magnitude response possesses octagonal symmetry [5]–[7]. Using the separable denominator transfer function in (2), the following constraints on the coefficients can be obtained as: $a_{ij} = a_{ji} =$

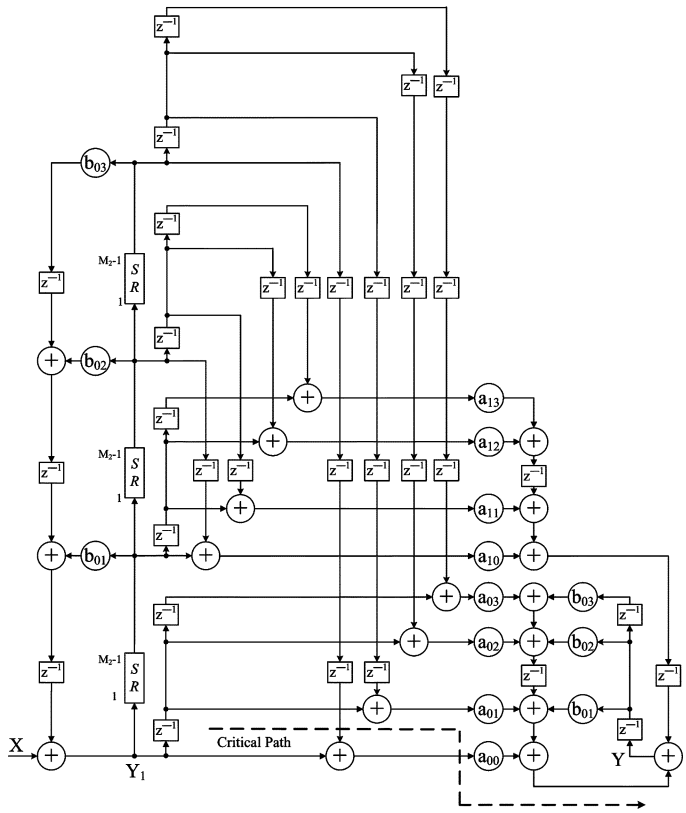

Fig. 7. Proposed Type-1 2-D quadrantal symmetry filter structure with separable denominator for $N = 3$.

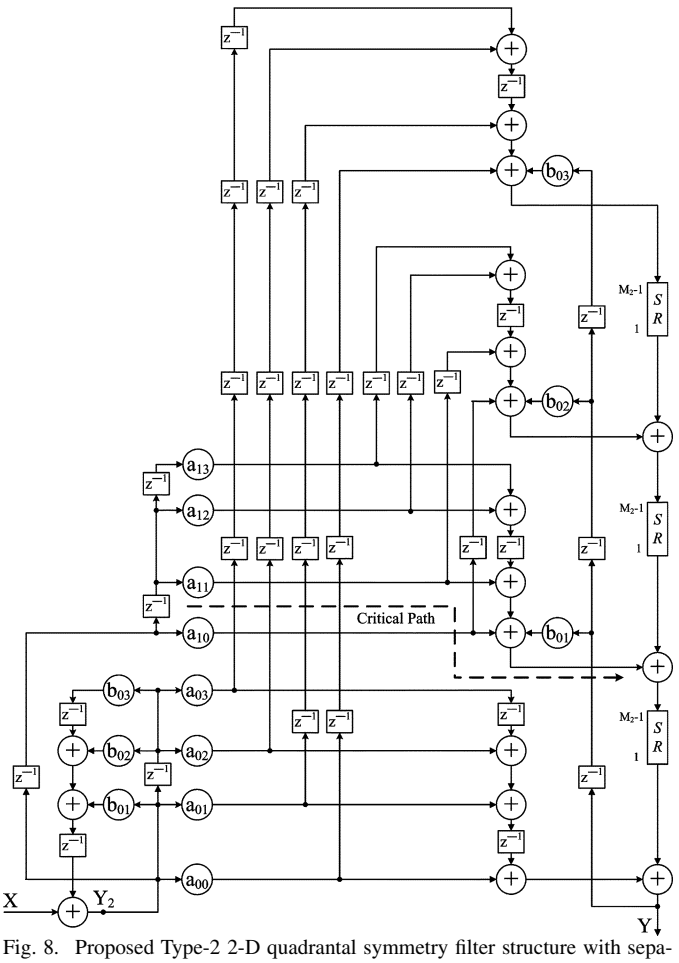

Fig. 8. Proposed Type-2 2-D quadrantal symmetry filter structure with separable denominator for $N = 3$.

$a_{(N-i)j}$ and $b_{k0} = b_{0k}$ for all i, j, k. Utilizing these constraints on the transfer function in (2), (4) and (5) can be recast in (15a) and (15b), respectively (see equation (15a)–(15b) at the bottom of the page) and (7) and (8) can be recast in (16a) and (16b), respectively (see equation (16a)–(16b) at the bottom of the next page). Considering the transfer function in (15a) and (15b) with $N = 3$, the Type-1 2-D octagonal symmetry filter structure with separable denominator is obtained in Fig. 9. Similarly, in accordance with (16a) and (16b) with $N = 3$, the Type-2 2-D octagonal symmetry filter structure with separable denominator is obtained in Fig. 10. Using the tree method to arrange the adders, the critical paths are analyzed as $T_m + 3T_a$ and $T_m + 2T_a$ as shown in Figs. 9 and 10, respectively. All eight cost-effective filter structures possess fewer multipliers, especially for the 2-D octagonal symmetry structures in Figs. 9 and 10 which have the lowest number of multipliers. The complete comparison is addressed in Section V.

Furthermore, concerning the symmetry filter structure for different order N, the generalized design procedure for the Type-1 symmetry filter is described as follows.

Step 1: Determine the filter order N and symmetry property.

Step 2: Determine the independent coefficients and transfer functions of Y_1/X and Y/Y_1 with specific value of N from the symmetry property.

Step 3: Depict the structure of the Type-1 separable denominator 2-D IIR filter with specific value of N (e.g., Fig. 1 with $N = 3$) and replace the corresponding dependent coefficients using the independent coefficient.

Step 4: According to the structure of the Type-1 separable denominator 2-D IIR filter and the transfer function of Y/Y_1, the delay arrangement equation in terms of the sum of delays associated with one independent numerator coefficient can be obtained.

Step 5: Based on the delay arrangement equation associated with the one independent numerator coefficient, the paths ahead of the replaced dependent coefficient multipliers in the Type-1 separable denominator 2-D IIR filter structure are cut and the cut signal paths are added into the path before the independent numerator coefficient multiplier. Then, the replaced dependent numerator coefficient multipliers can be removed.

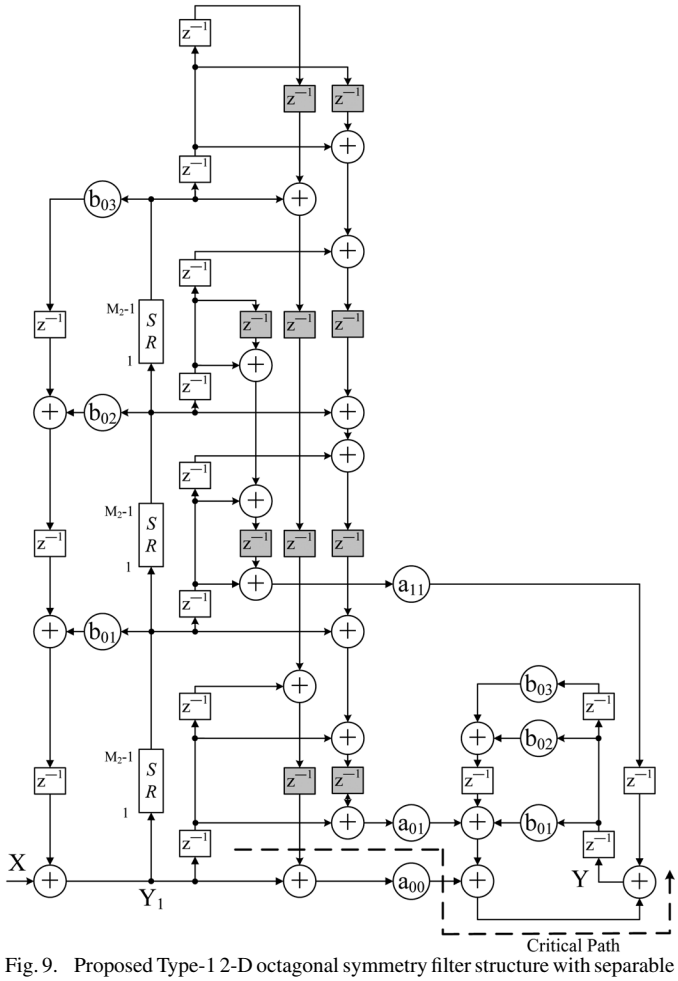

Fig. 9. Proposed Type-1 2-D octagonal symmetry filter structure with separable denominator for $N = 3$.

$$Y_1 = X + \sum_{j=1}^{N} b_{0j} z_1^{-j} Y_1 \tag{15a}$$

$$\begin{aligned} Y = {} & \sum_{j=1}^{N} b_{0j} z_2^{-j} Y + v a_{uu} z_1^{-u} z_2^{-u} Y_1 \\ & + v \cdot \sum_{i=0}^{u-v} a_{iu} \left(z_1^{-i} z_2^{-u} + z_1^{-u} z_2^{-(N-i)} + z_1^{-(N-i)} z_2^{-(N-u)} + z_1^{-(N-u)} z_2^{-i} \right) Y_1 \\ & + \sum_{i=0}^{u-v} a_{ii} \left(z_1^{-i} z_2^{-i} + z_1^{-i} z_2^{-(N-i)} + z_1^{-(N-i)} z_2^{-(N-i)} + z_1^{-(N-i)} z_2^{-i} \right) Y_1 \\ & + \sum_{i=0}^{u-v-1} \sum_{j=i+1}^{u-v} a_{ij} \Bigg(z_1^{-i} z_2^{-j} + z_1^{-i} z_2^{-(N-j)} + z_1^{-(N-i)} z_2^{-j} + z_1^{-(N-i)} z_2^{-(N-j)} + z_1^{-j} z_2^{-i} \\ & \qquad + z_1^{-j} z_2^{-(N-i)} + z_1^{-(N-j)} z_2^{-i} + z_1^{-(N-j)} z_2^{-(N-i)} \Bigg) Y_1 \end{aligned} \tag{15b}$$

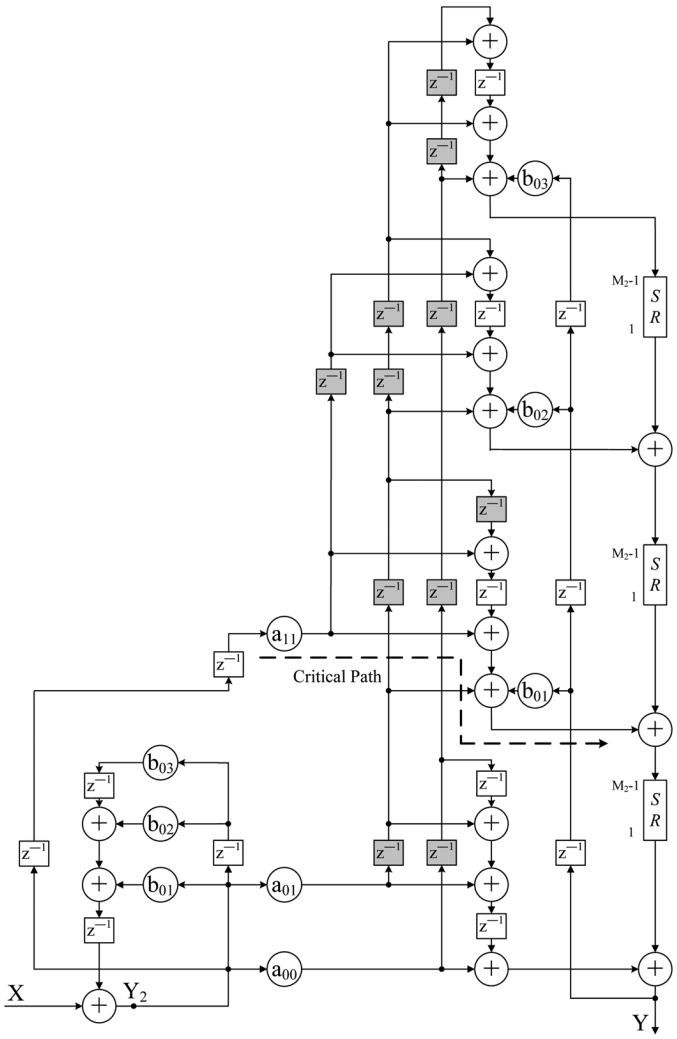

Fig. 10. Proposed Type-2 2-D octagonal symmetry filter structure with separable denominator for $N = 3$.

Step 6: Repeat Step 4 and Step 5 for the rest of the independent numerator coefficients.

Step 7: Remove the resulting unnecessary adders (i.e., the adder with single input or no input source) and the resulting unnecessary delay elements (i.e., the delay with no input source or output destination).

Similarly, the above generalized design procedure can be applied to the Type-2 symmetry filter with the modifications to Step 2, Step 3, Step 4, and Step 5 as described below.

Step 2: Determine the independent coefficients and transfer functions of Y_2/X and Y/Y_2 with specific value of N from the symmetry property.

Step 3: Depict the structure of the Type-2 separable denominator 2-D IIR filter with specific value of N (e.g., Fig. 2 with $N = 3$) and replace the corresponding dependent coefficients using the independent coefficient.

Step 4: According to the structure of the Type-2 separable denominator 2-D IIR filter and the transfer function of Y/Y_2, the delay arrangement equation in terms of the sum of delays associated with one independent numerator coefficient can be obtained.

Step 5: Based on the delay arrangement equation associated with the one independent numerator coefficient, the paths after the independent coefficient multiplier in the Type-2 separable denominator 2-D IIR filter structure are branched and the branched signal paths are added into the path behind the replaced dependent numerator coefficient multipliers. Then, the replaced dependent numerator coefficient multipliers can be removed.

To illustrate, we will use the above procedure to obtain the Type-1 and Type-2 octagonal symmetry filter structures with $N = 3$ in Figs. 9 and 10, respectively. In the first example, the Type-1 octagonal symmetry filter structure with $N = 3$ is illustrated as follows. In Step 1, we select the Type-1 octagonal symmetry filter order to be $N = 3$. In Step 2, according to octagonal symmetry property, we can determine that a_{00}, a_{01}, a_{11}, b_{01}, b_{02}, b_{03} are independent coefficients and the others are dependent coefficients. Thus, the transfer functions of Y_1/X and Y/Y_1 with $N = 3$ can be obtained from (15a) and (15b), respectively. In Step 3, the structure of the Type-1 separable

$$Y_2 = X + \sum_{j=1}^{N} b_{0j} z_2^{-j} Y_2 \tag{16a}$$

$$\begin{aligned} Y = {} & \sum_{j=1}^{N} b_{0j} z_1^{-j} Y + v a_{uu} z_1^{-u} z_2^{-u} Y_2 \\ & + v \cdot \sum_{i=0}^{u-v} a_{iu} \left(z_1^{-i} z_2^{-u} + z_1^{-u} z_2^{-(N-i)} + z_1^{-(N-i)} z_2^{-(N-u)} + z_1^{-(N-u)} z_2^{-i} \right) Y_2 \\ & + \sum_{i=0}^{u-v} a_{ii} \left(z_1^{-i} z_2^{-i} + z_1^{-i} z_2^{-(N-i)} + z_1^{-(N-i)} z_2^{-(N-i)} + z_1^{-(N-i)} z_2^{-i} \right) Y_2 \\ & + \sum_{i=0}^{u-v-1} \sum_{j=i+1}^{u-v} a_{ij} \Big(z_1^{-i} z_2^{-j} + z_1^{-i} z_2^{-(N-j)} + z_1^{-(N-i)} z_2^{-j} + z_1^{-(N-i)} z_2^{-(N-j)} \\ & \qquad + z_1^{-j} z_2^{-i} + z_1^{-j} z_2^{-(N-i)} + z_1^{-(N-j)} z_2^{-i} + z_1^{-(N-j)} z_2^{-(N-i)} \Big) Y_2 \end{aligned} \tag{16b}$$

denominator 2-D IIR filter with order $N = 3$ can be easily obtained in Fig. 1. Then, the dependent coefficients are replaced by the corresponding independent coefficients. In Step 4, for the case of the a_{01} independent numerator coefficient, since $a_{01} = a_{02} = a_{10} = a_{13} = a_{20} = a_{23} = a_{31} = a_{32}$, the sum of delay terms associated with a_{01} in (15b) with $N = 3$ can be expressed in (17a)

$$S_{1,a_{01}} = a_{01}\Big(z_2^{-1}+z_2^{-2}+z_1^{-1}+z_1^{-1}z_2^{-3}+z_1^{-2} +z_1^{-2}z_2^{-3}+z_1^{-3}z_2^{-1}+z_1^{-3}z_2^{-2}\Big)Y_1 \tag{17a}$$

where $S_{1,a01}$ denotes the sum of delay terms associated with a_{01} in the Type-1 octagonal symmetry filter. According to the structure of the Type-1 separable denominator 2-D IIR filter in Fig. 1, eight delay terms in the square brackets in (17b) denote the delays of the unchanged signal paths in the Type-1 octagonal symmetry filter. That means these eight delay terms in the square brackets are fixed for delay arrangement

$$\begin{aligned} S_{1,a_{01}} = a_{01}\Big(&\left[z_2^{-1}\right] + z_2^{-1}\left[z_2^{-1}\right] + z_2^{-1}\left[z_1^{-1}z_2^{1}\right] \\ &+ z_2^{-2}\left[z_1^{-1}z_2^{-1}\right] + z_2^{-2}\left[z_1^{-2}z_2^{2}\right] + z_2^{-3}\left[z_1^{-2}\right] \\ &+ z_2^{-3}\left[z_1^{-3}z_2^{2}\right] + z_2^{-4}\left[z_1^{-3}z_2^{2}\right]\Big)Y_1 \end{aligned} \tag{17b}$$

The other delays before the square brackets in (17b), however, are adjustable for delay arrangement. After extracting the shared delay elements, (17b) can be recast in (17c) (shown at the bottom of the page). Here, (17c) is referred to as the delay arrangement equation for the a_{01} independent coefficient. In Step 5, according to (17c), seven cut signal paths ahead of the replaced dependent coefficient multipliers $\{a_{02}, a_{10}, a_{13}, a_{20}, a_{23}, a_{31}, a_{32}\}$ are rearranged and summed into the path before the a_{01} independent coefficient multiplier. The replaced dependent coefficient multipliers are then removed. In (17c), the signal paths are added ahead of the a_{01} independent coefficient multiplier and the delay elements before each parenthesis are shown as rightmost-column gray delay elements in Fig. 9. In Step 6, for the rest of the independent numerator coefficients a_{00} and a_{11}, repeat Step 4 and Step 5, the delay arrangement equations and gray delay elements can be obtained. Finally, the resulting unnecessary adders and delay elements are removed to obtain the 2-D octagonal symmetry filter structure in Fig. 9. Note that, in other independent numerator coefficient cases, if no delay element can be shared in (17b), (17c) will be the same as (17b).

In the second example, the Type-2 octagonal symmetry filter structure with $N = 3$ is illustrated as follows. In Step 1, we select the Type-2 octagonal symmetry filter order to be $N = 3$. In Step 2, due to the same symmetry property as that in the previous example, we can determine that a_{00}, a_{01}, a_{11}, b_{01}, b_{02}, b_{03} are independent coefficients and the others are dependent coefficients. Thus, the transfer functions of Y_2/X and Y/Y_2 with $N = 3$ can be obtained from (16a) and (16b), respectively. In Step 3, the structure of the Type-2 separable denominator 2-D IIR filter with order $N = 3$ can be easily obtained in Fig. 2. Then, the dependent coefficients are replaced by the corresponding independent coefficients. In Step 4, the sum of the delay terms associated with a_{01} can be expressed in (18a)

$$\begin{aligned} S_{2,a_{01}} = a_{01}(&z_2^{-1} + z_2^{-2} + z_1^{-1} + z_1^{-1}z_2^{-3} + z_1^{-2} \\ &+ z_1^{-2}z_2^{-3} + z_1^{-3}z_2^{-1} + z_1^{-3}z_2^{-2})Y_2 \end{aligned} \tag{18a}$$

where $S_{2,a01}$ denotes the sum of delay terms associated with a_{01} in the Type-2 octagonal symmetry filter. According to the structure of the Type-2 separable denominator 2-D IIR filter in Fig. 2, eight delay terms in the square brackets in (18b) denote the delays of the unchanged signal paths in the Type-2 octagonal symmetry filter. That means these eight delay terms in the square brackets are fixed for delay arrangement

$$\begin{aligned} S_{2,a_{01}} = a_{01}\Big(&\left[z_2^{-1}\right] + z_2^{-1}\left[z_2^{-1}\right] + z_2^{-1}\left[z_1^{-1}z_2^{1}\right] \\ &+ z_2^{-3}\left[z_1^{-1}\right] + z_2^{-2}\left[z_1^{-2}z_2^{2}\right] + z_2^{-4}\left[z_1^{-2}z_2^{1}\right] \\ &+ z_2^{-4}\left[z_1^{-3}z_2^{3}\right] + z_2^{-4}\left[z_1^{-3}z_2^{2}\right]\Big)Y_2. \end{aligned} \tag{18b}$$

The other delays before the square brackets in (18b), however, are adjustable for delay arrangement. After extracting the shared delay elements, (18b) can be recast in (18c) (shown at the bottom of the next page). Here, (18c) is referred to as the delay arrangement equation for the a_{01} independent coefficient. In Step 5, according to (18c), the signal paths are dispatched after the a_{01} independent coefficient multiplier and the delay elements before each parenthesis are shown as gray delay elements associated with a_{01} in Fig. 10. In the same manner, the delay arrangement equations and gray delay elements corresponding to independent numerator coefficients a_{00} and a_{11} can be obtained in Step 6. Finally, the resulting unnecessary adders and delay elements are removed to obtain the 2-D octagonal symmetry filter structure in Fig. 10.

$$\begin{aligned} S_{1,a_{01}} = a_{01}\Big(&\left[z_2^{-1}\right] + z_2^{-1}\Big(\left[z_2^{-1}\right] \\ &+ \left[z_1^{-1}z_2^{1}\right] + z_2^{-1}\Big(\left[z_1^{-1}z_2^{-1}\right] + \left[z_1^{-2}z_2^{2}\right] \\ &+ z_2^{-1}\left(\left[z_1^{-2}\right] + \left[z_1^{-3}z_2^{2}\right] + z_2^{-1}\left(\left[z_1^{-3}z_2^{2}\right]\right)\right)\Big)\Big)\Big)Y_1 \end{aligned} \tag{17c}$$

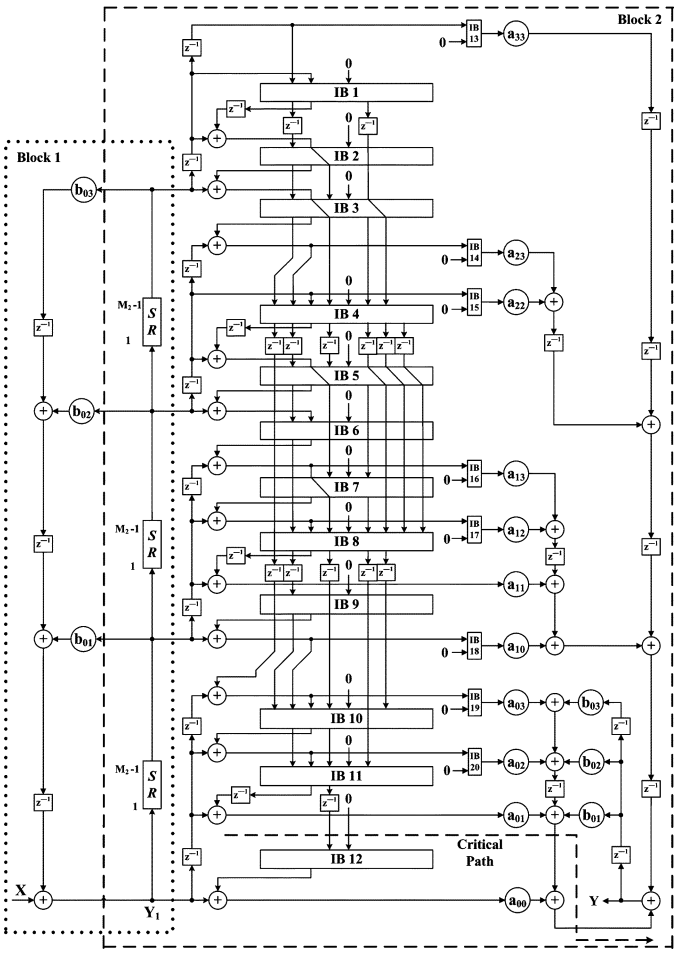

Fig. 11. Proposed multimode 2-D filter architecture with four symmetries for $N = 3$.

In Figs. 9 and 10, it can be observed that although the numbers of delays of the same independent numerator coefficient for the Type-1 and Type-2 octagonal symmetry filters are the same, the gray delay element arrangement of the Type-2 octagonal symmetry filter in Fig. 10 is more complicated than that of the Type-1 octagonal symmetry filter in Fig. 9 for $N = 3$. In the same way, the other six symmetry filters can be analyzed. It can be observed that the gray delay element arrangements of the Type-2 fourfold rotational and quadrantal symmetry filters are complicated compared with that of the Type-1 fourfold rotational and quadrantal symmetry filters for $N = 3$. The similar approach can be followed for any order N for all the symmetries.

$$\begin{bmatrix} a_{00} & a_{01} & a_{02} & a_{03} \\ a_{10} & a_{11} & a_{12} & a_{13} \\ a_{20} & a_{21} & a_{22} & a_{23} \\ a_{30} & a_{31} & a_{32} & a_{33} \end{bmatrix} \quad \text{(a)}$$

$$\begin{bmatrix} a_{00} & a_{01} & a_{02} & a_{03} \\ a_{01} & a_{11} & a_{12} & a_{13} \\ a_{02} & a_{12} & a_{22} & a_{23} \\ a_{03} & a_{13} & a_{23} & a_{33} \end{bmatrix} \quad \text{(b)}$$

$$\begin{bmatrix} a_{00} & a_{01} & a_{02} & a_{00} \\ a_{02} & a_{11} & a_{11} & a_{01} \\ a_{01} & a_{11} & a_{11} & a_{02} \\ a_{00} & a_{02} & a_{01} & a_{00} \end{bmatrix} \quad \text{(c)}$$

$$\begin{bmatrix} a_{00} & a_{01} & a_{02} & a_{03} \\ a_{10} & a_{11} & a_{12} & a_{13} \\ a_{10} & a_{11} & a_{12} & a_{13} \\ a_{00} & a_{01} & a_{02} & a_{03} \end{bmatrix} \quad \text{(d)}$$

$$\begin{bmatrix} a_{00} & a_{01} & a_{01} & a_{00} \\ a_{01} & a_{11} & a_{11} & a_{01} \\ a_{01} & a_{11} & a_{11} & a_{01} \\ a_{00} & a_{01} & a_{01} & a_{00} \end{bmatrix} \quad \text{(e)}$$

Fig. 12. Coefficient distributions of the numerators in matrix form for: (a) general filter; (b) DSM mode; (c) FRSM mode; (d) QSM mode; (e) OSM mode.

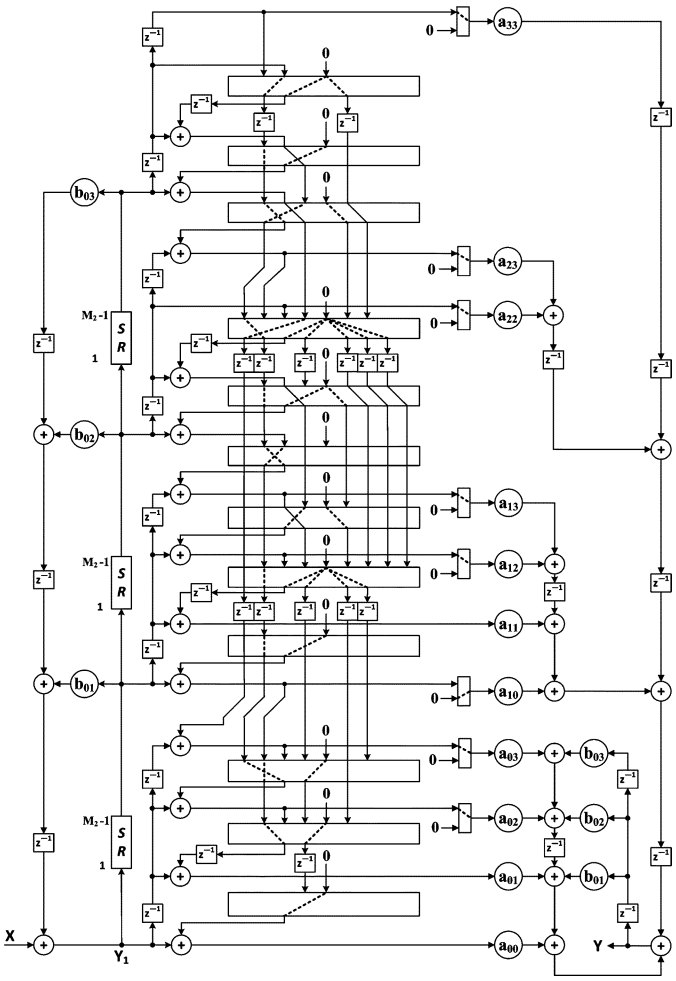

Fig. 13. Diagonal symmetry mode (DSM) operation of the proposed multimode filter for $N = 3$.

$$S_{2,a_{01}} = a_{01}\left(\left[z_2^{-1}\right] + z_2^{-1}\left(\left[z_2^{-1}\right] + \left[z_1^{-1}z_2^{1}\right] + z_2^{-1}\left(z_2^{-1}\left(\left[z_1^{-1}\right]\right) + \left[z_1^{-2}z_2^{2}\right] + z_2^{-2}\left(\left[z_1^{-2}z_2^{1}\right] + \left[z_1^{-3}z_2^{3}\right] + \left[z_1^{-3}z_2^{2}\right]\right)\right)\right)\right)Y_2 \tag{18c}$$

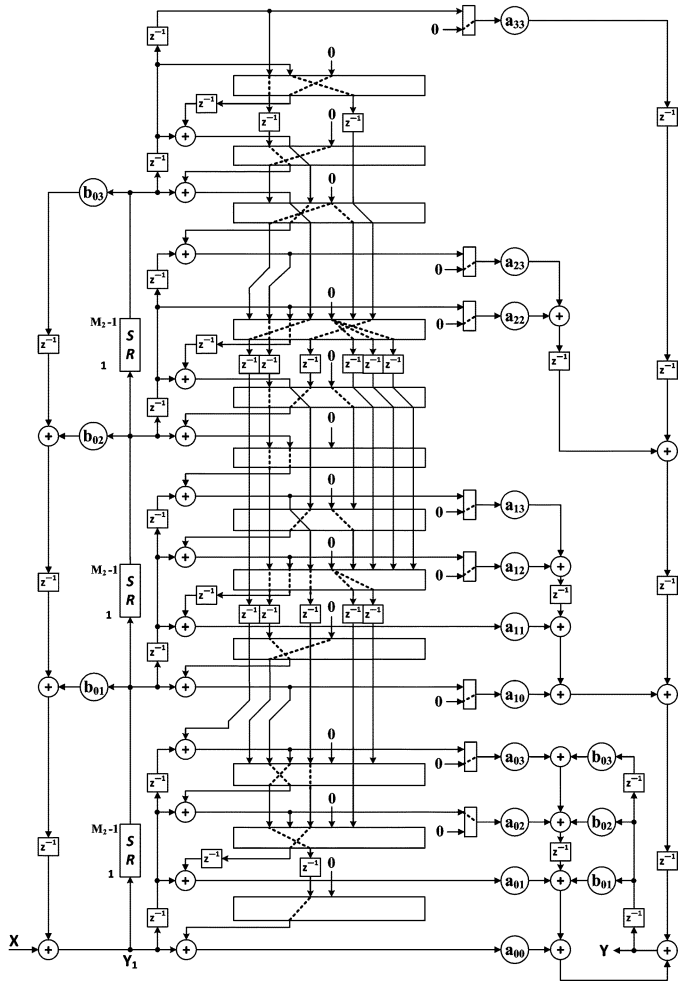

Fig. 14. Fourfold rotational symmetry mode (FRSM) operation of the proposed multimode filter for $N = 3$.

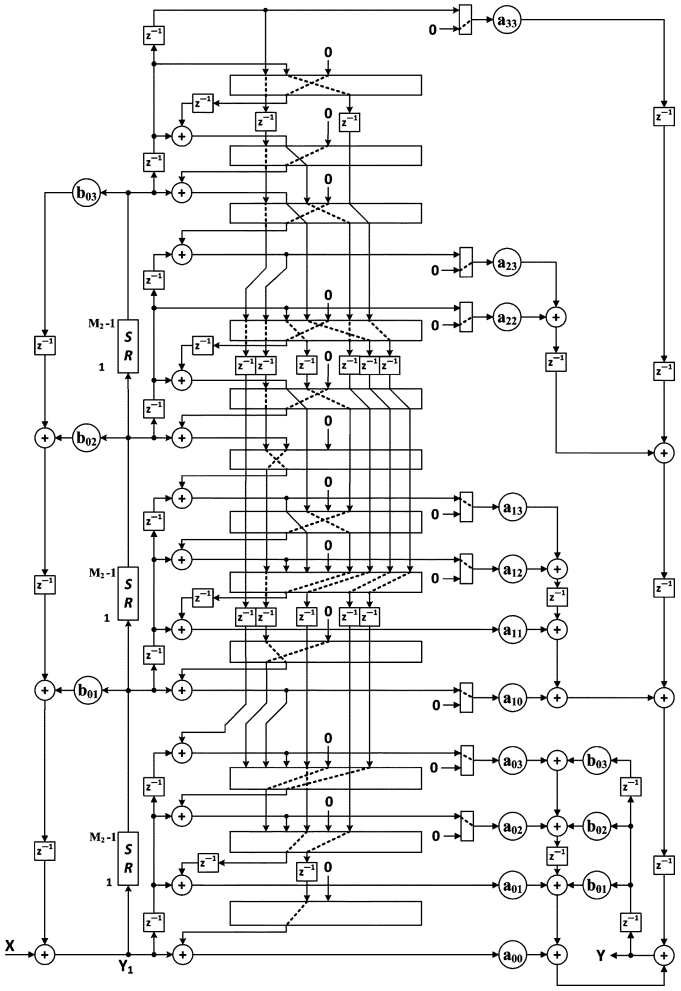

Fig. 15. Quadrantal symmetry mode (QSM) operation of the proposed multimode filter for $N = 3$.

IV. Cost-Effective Multimode 2-D Filter Architecture With Four Symmetries

In order to support multiple symmetry functions, we propose one cost-effective multimode 2-D filter design with four symmetry modes: diagonal symmetry mode (DSM), fourfold rotational symmetry mode (FRSM), quadrantal symmetry mode (QSM), and octagonal symmetry mode (OSM). The cost-effective multimode 2-D symmetry filter architecture with $N = 3$ shown in Fig. 11 can be obtained based on the following three observations.

First, it is observed that signal paths are added before the a_{ij} independent coefficient multiplier for the Type-1 symmetry filters in Figs. 3, 5, 7, and 9, and signal paths are dispatched after the a_{ij} independent coefficient multiplier for the Type-2 symmetry filters in Figs. 4, 6, 8, and 10. From the delay arrangement analysis in Section III, the Type-2 fourfold rotational, quadrantal, and octagonal symmetry filters have more complicated delay arrangement for $N = 3$. Thus, the four Type-1 symmetry structures are selected for the proposed multimode 2-D filter as the basis for the four configuration modes.

Second, it can be observed in (3) that the Type-1 symmetry filter consists of two transfer functions: Y_1/X and Y/Y_1, with the Y_1/X transfer function being the same for the four individual symmetry filters as shown in (9a), (11a), (13a), and (15a). The block diagram of Y_1/X is depicted as Block 1 on the left hand side of Fig. 11. Block 1 requires 3 multipliers and 3 adders. Next, we consider the Y/Y_1 transfer function which is different for each of the four individual symmetry filters. To construct Block 2 of the multimode filter, we need 3 multipliers for the denominator $\{b_{01}, b_{02}, b_{03}\}$, and 11 multipliers for the numerator. To illustrate the requirements on the numerator multipliers, we use the matrix format to show the numerator coefficient distribution. The numerator coefficient distribution of the general filter is shown in Fig. 12(a). The four numerator coefficient distributions for the DSM, FRSM, QSM, and OSM modes are expressed in Fig. 12(b)–(e), respectively. It can be seen that due to symmetry, not all the coefficients are independent. The DSM and FRSM modes require 10 and 4 independent coefficient multipliers for their numerators respectively, while the QSM and OSM modes require 8 and 3 coefficient multipliers for their numerators. Thus, the union set of the independent coefficients is $\{a_{00}, a_{01}, a_{02}, a_{03}, a_{10}, a_{11}, a_{12}, a_{13}, a_{22}, a_{23}, a_{33}\}$. Therefore, $11 + 3 = 14$ coefficient multipliers are required in Block 2 of Fig. 11 to achieve the operations for four different transfer functions of Y/Y_1. We next consider the number of adders. From the architecture viewpoint, for Y/Y_1 of the multimode 2-D symmetry filter, 13 adders and 11 adders are needed on the left hand side and right hand side of Block 2 in Fig. 11, respectively. The former number can be determined by the Type-1 octagonal symmetry filter structure in Fig. 9. The latter number can be determined by the Type-1 diagonal and quadrantal symmetry filters

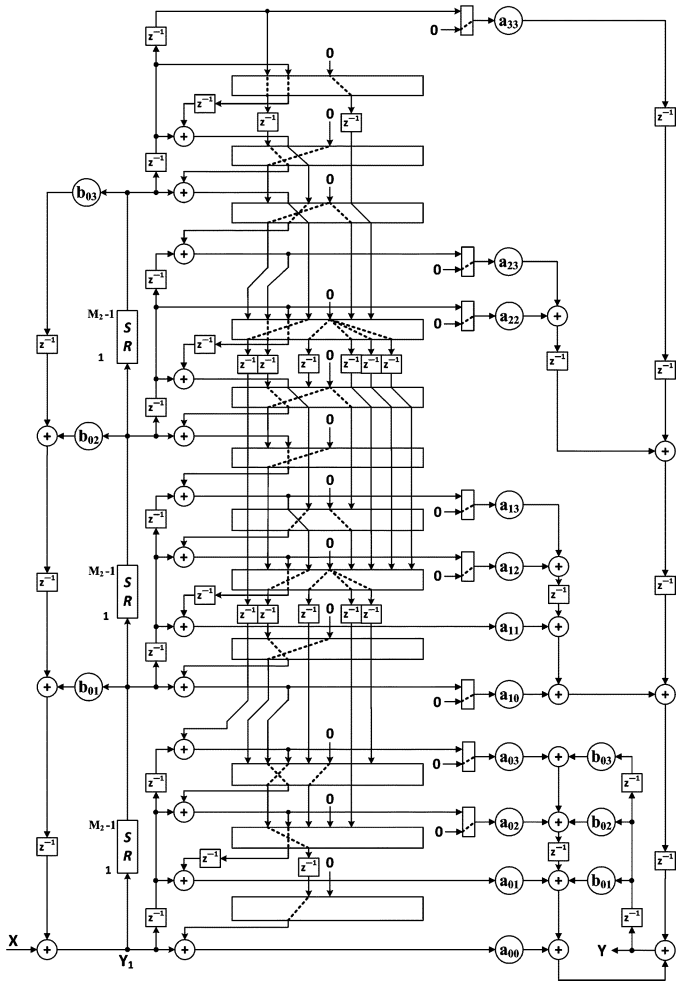

Fig. 16. Octagonal symmetry mode (OSM) operation of the proposed multimode filter for $N = 3$.

in Figs. 3 and 7, respectively. In summary, the proposed multimode 2-D symmetry filter requires altogether 17 coefficient multipliers and 27 adders as shown in Fig. 11.

Third, in Figs. 3, 5, 7, and 9, the interconnection control is only needed for the four Y/Y_1 transfer functions. The multiplication connections and internal connections are controlled by interconnection boxes (IBs) to accomplish the four-mode operations, where IB performs either connection or disconnection task for each signal path. According to the connections of the four individual symmetry filter structures, 12 IBs are needed for the internal connections in Block 2. Note that the solid line feeding through the IB means that this signal path is not controlled by four modes. On the other hand, for the multiplication connection control, only 8 IBs are needed for $N = 3$.

As a consequence, considering the three observations mentioned above, the multimode 2-D filter with four symmetry modes can be obtained in Fig. 11. The multimode filter architecture has a critical path of $T_m + 3T_a$ as shown in Fig. 11 by using the tree method. The corresponding signal path connections of DSM, FRSM, QSM, and OSM are presented in Figs. 13–16, respectively, where the dash lines denote the different connections within each IB for each mode. The difference in the interconnections for the four modes of the proposed multimode filter is highlighted in Fig. 17. Since we only use one hardware resource with a slight area overhead to support four different symmetry modes, the proposed structure achieves an area reduction of 63.25% compared with the sum

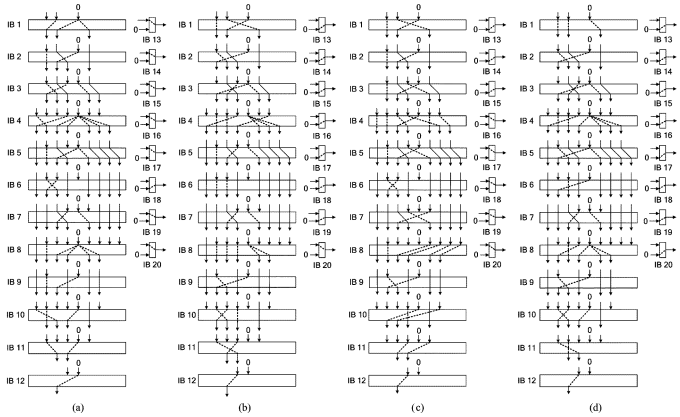

Fig. 17. Interconnections of: (a) DSM; (b) FRSM; (c) QSM; (d) OSM for $N = 3$.

of the areas of the four individual symmetry filter structures. Hence, the proposed structure is cost effective.

V. Comparison and Evaluation Results

The architecture analysis results are shown in Table I in terms of the number of multipliers and critical path for $N = 3$. This work proposes eight novel individual 2-D symmetry filters and one multimode 2-D symmetry filter. The Type-1 symmetry filters possess simple delay arrangement and the Type-2 symmetry filters have shorter critical path. Among these filters, the proposed Type-1 and Type-2 octagonal symmetry filters have the lowest number of multipliers.

Most importantly, the power and core area evaluation results among the proposed four Type-1 2-D individual symmetry filter architectures, one multimode 2-D symmetry filter architecture, one Type-1 2-D separable denominator filter architecture, and other referenced filter architectures are presented in Table II. Here, all evaluated filter architectures with $N = 3$ and $M_2 = 8$ have been implemented in TSMC 0.18 μm general-purpose one-poly six-metal (1P6M) CMOS process with 1.8-V Artisan standard cell library. The wordlengths of the filter input, filter output, coefficients, and register outputs are 10, 10, 16, and 16 bits, respectively. The 16×16-bit multiplier is adopted for the proposed 2-D symmetry filters, multimode filter, and separable denominator filter.

For the 2-D conventional filter [12], the 10×16-bit and 16×16-bit multipliers are used for the coefficient multiplications of a_{ij} and b_{ij}, respectively. Although the conventional filter has the largest number of multipliers, it is expected that the power and area of the filter can be reduced due to the use of 10×16-bit multiplier. In order to save the number of coefficient inputs for the filter implementation, the coefficients are loaded sequentially through one 16-bit coefficient input and stored in the individual registers. After the coefficients of register are loaded into the corresponding multipliers in parallel, the filter begins to work. In this manner, the requirement of the number of pads can be significantly reduced.

The cell-based design flow is adopted for the chip implementation and addressed as follows. Synopsys Design Compiler is employed to synthesize the proposed and referenced 2-D filter designs in RTL level and Cadence SOC Encounter is adopted for placement and routing (P&R). The power dissipation is measured via Synopsys PrimePower using 100 000 combinations of random vectors after RC extraction of the placed and routed netlists at 100 MHz. The 100 000 combinations is composed of 100-set stable coefficients by 1000 random inputs per each

TABLE I
COMPARISON RESULTS AMONG THE 2-D IIR DIGITAL FILTER ARCHITECTURES

2-D Filter Architecture		No. of Multipliers	Critical Path for N=3
Ahmed [10]		$2(N+1)^2-1$	$T_m+(2+\lceil\log_2(N+1)\rceil)T_a$
Van [12]		$2(N+1)^2-1$	T_m+3T_a
Separable denominator filter [13]	Type-1	$(N+1)^2+2N$	T_m+3T_a
	Type-2	$(N+1)^2+2N$	T_m+2T_a
Non-separable denominator filter [14, 15]	Diagonal symmetry	$(N+1)^2+N$	T_m+2T_a
	Four-fold rotational symmetry	$\frac{3}{4}(N+1)^2+\frac{1}{2}(N+1)-1$	T_m+3T_a
Proposed diagonal symmetry filter	Type-1	$\frac{1}{2}(N+1)^2+\frac{5}{2}N+\frac{1}{2}$	T_m+3T_a
	Type-2 [13]	$\frac{1}{2}(N+1)^2+\frac{5}{2}N+\frac{1}{2}$	T_m+2T_a
Proposed four-fold rotational symmetry filter	Type-1	$\frac{1}{4}(N+1)^2+\frac{3}{4}v+2N$	T_m+3T_a
	Type-2	$\frac{1}{4}(N+1)^2+\frac{3}{4}v+2N$	T_m+2T_a
Proposed quadrantal symmetry filter	Type-1	$\frac{1}{2}(N+1)^2+\frac{v}{2}(N+1)+2N$	T_m+3T_a
	Type-2	$\frac{1}{2}(N+1)^2+\frac{v}{2}(N+1)+2N$	T_m+2T_a
Proposed octagonal symmetry filter	Type-1	$\frac{1}{8}(N+1+v)^2+\frac{1}{4}(N+1+v)+2N$	T_m+3T_a
	Type-2	$\frac{1}{8}(N+1+v)^2+\frac{1}{4}(N+1+v)+2N$	T_m+2T_a
Proposed multimode symmetry filter	Type-1	$\frac{1}{2}(N+1)^2+\frac{1}{2}(N+1)+\frac{1}{8}(N+1+v)^2-\frac{1}{4}(N+1+v)+2N$	T_m+3T_a

TABLE II
EVALUATION RESULTS OF 2-D IIR DIGITAL FILTER ARCHITECTURES

2-D Filter Architecture		Power Consumption		Core Area	
Conventional filter [12]		38.51 mW	100%	608,703 um^2	100%
Proposed Type-1 separable denominator filter [13]		34.62 mW	89.90%	528,099 um^2	86.76%
Proposed Type-1 diagonal symmetry filter		32.05 mW	83.23%	418,608 um^2	68.77%
Proposed Type-1 four-fold rotational symmetry filter		24.53 mW	63.70%	291,381 um^2	47.87%
Proposed Type-1 quadrantal symmetry filter		29.69 mW	77.10%	393,384 um^2	64.63%
Proposed Type-1 octagonal symmetry filter		23.98 mW	62.27%	287,592 um^2	47.25%
Proposed multimode symmetry filter architecture	DSM	34.27 mW	88.99%	511,209 um^2	83.98%
	FRSM	26.41 mW	68.58%		
	QSM	31.76 mW	82.47%		
	OSM	24.93 mW	64.74%		
	Average	29.34 mW	76.19%	511,209 um^2	83.98%

set stable coefficient. From Table II, it can be seen that the presented four individual symmetry filter structures are capable of providing low power and low area consumption.

In terms of power consumption, the diagonal, fourfold rotational, quadrantal, and octagonal symmetry filter structures can attain power savings of 16.77%, 36.30%, 22.90%, and 37.73% with respect to that of the conventional filter architecture [12], and power savings of 7.42%, 29.15%, 14.24%, and 30.73% with respect to that of the Type-1 separable denominator filter architecture [13]. On the other hand, the layout of the proposed multimode 2-D filter for $N = 3$ in Fig. 11 is shown in Fig. 18 with the area size of $718.95\ \mu\text{m} \times 711.05\ \mu\text{m}$. The corresponding power consumption of the proposed multimode 2-D filter is 29.34 mW on average. In terms of power comparison, the DSM, FRSM, QSM, and OSM modes can attain power reductions of 11.01%, 31.42%, 17.53%, and 35.26% with respect to that of the conventional filter architecture [12], and power reductions of 1.01%, 23.71%, 8.26%, and 27.99% with respect to that of the Type-1 separable denominator filter architecture [13]. Compared with the four individual symmetry filter designs, the corresponding modes of the multimode architecture increase the power consumption by 6.93%, 7.66%, 6.97%, and 3.96%, respectively. Although each individual symmetry filter structure has smaller area and lower power consumption than the proposed multimode filter architecture does, these four individual symmetry filter structures are single-mode such that each of them cannot be applied to the demand of a multiple-symmetry system. So the multimode filter architecture can save more chip area when the

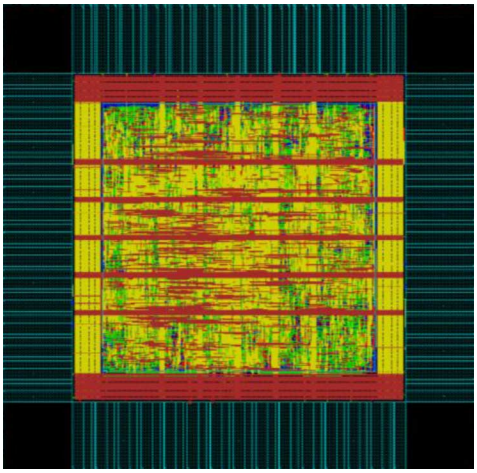

Fig. 18. Layout of the proposed multimode symmetry filter for $N = 3$.

four individual symmetry filter structures are needed in a multiple-symmetry system. Compared with the sum of the areas of the four individual symmetry filters, the area saving could be up to 63.25%. Hence, the proposed multimode filter architecture is power efficient and cost effective.

VI. Conclusion

In this paper, eight new power-efficient and cost-effective individual 2-D symmetry filter structures and one multimode filter with diagonal, fourfold rotational, quadrantal and octagonal symmetry modes are presented for a 2-D filter transfer function of order 3×3. By using the developed generalized design procedure, the individual symmetry filter structure for different order could be obtained. Further, it is to be noted that the symmetry conditions imposed are the sufficient conditions for the existence of those symmetries in a given transfer function. The novel aspect of the work is taking into account the presence of symmetry in the 2-D VLSI filter implementation and thereby reducing the power and the cost of the design. From the implementation results, the proposed four symmetry structures can attain power savings of 16.77%, 36.30%, 22.90%, and 37.73% with respect to that of the conventional filter architecture [12], and the power savings of 7.42%, 29.15%, 14.24%, and 30.73% with respect to that of the Type-1 separable denominator filter architecture [13]. On the other hand, the proposed multimode filter architecture can attain the power reduction on average by 15.25% with respect to that of the Type-1 separable denominator filter architecture. It will be of interest to study and compare various 2-D digital filter structures possessing different magnitude symmetries. In [17], the work on the generalized formulation of 2-D filter structures with symmetry is initiated.

References

[1] M. Petrou and P. Bosdogianni, *Image Processing*. New York: Wiley, 2000.

[2] A. M. Tekalp, *Digital Video Processing*. Englewood Cliffs, NJ: Prentice-Hall, 1995, ch. 14.

[3] M. A. Sid-Ahmed, *Image Processing: Theory, Algorithms, and Architectures*. New York: McGraw-Hill, 1995.

[4] D. E. Dudgeon and R. M. Mersereau, *Multidimensional Digital Signal Processing*. Englewood Cliffs, NJ: Prentice-Hall, 1984.

[5] M. N. S. Swamy and P. K. Rajan, "Symmetry in 2-D filters and its application," in *Multidimensional Systems: Techniques and Applications*, S. Tzafestas, Ed. New York: Marcel Dekkar, 1986, ch. 9.

[6] H. C. Reddy, I. H. Khoo, and P. K. Rajan, "Application of symmetry: 2-D polynomials, fourier transform, and filter design," in *The Circuits and Filters Handbook*, W. K. Chen, Ed., 3rd ed. Boca Raton, FL: CRC, 2009.

[7] H. C. Reddy, I. H. Khoo, and P. K. Rajan, "2-D symmetry: Theory and filter design applications," *IEEE Circuits Syst. Mag.*, vol. 3, no. 3, pp. 4–33, 3rd Q., 2003.

[8] H. L. P. A. Madanayake and L. T. Bruton, "A speed-optimized systolic array processor architecture for spatio-temporal 2-D IIR broadband beam filter," *IEEE Trans. Circuits Syst. I, Reg. Papers*, vol. 55, no. 7, pp. 1953–1966, Aug. 2008.

[9] H. L. P. A. Madanayake, S. V. Hum, and L. T. Bruton, "A systolic array 2-D IIR broadband RF beamformer," *IEEE Trans. Circuits Syst. II, Exp. Briefs*, vol. 55, no. 12, pp. 1244–1248, Dec. 2008.

[10] M. A. Sid-Ahmed, "A systolic realization for 2-D digital filters," *IEEE Trans. Acoust., Speech, Signal Process.*, vol. 37, no. 4, pp. 560–565, Apr. 1989.

[11] N. R. Shanbhag, "An improved systolic architecture for 2-D digital filters," *IEEE Trans. Signal Process.*, vol. 39, no. 5, pp. 1195–1202, May 1991.

[12] L. D. Van, "A new 2-D systolic digital filter architecture without global broadcast," *IEEE Trans. Very Large Scale Integr. (VLSI) Syst.*, vol. 10, no. 4, pp. 477–486, Aug. 2002.

[13] I. H. Khoo, H. C. Reddy, L. D. Van, and C. T. Lin, "2-D digital filter architectures without global broadcast and some symmetry applications," in *Proc. IEEE ISCAS*, May 2009, pp. 952–955.

[14] P. Y. Chen, L. D. Van, H. C. Reddy, and C. T. Lin, "A new VLSI 2-D diagonal-symmetry filter architecture design," in *Proc. IEEE APCCAS*, Macao, China, Nov. 2008, pp. 320–323.

[15] P. Y. Chen, L. D. Van, H. C. Reddy, and C. T. Lin, "A new VLSI 2-D fourfold-rotational-symmetry filter architecture design," in *Proc. IEEE ISCAS*, May 2009, pp. 93–96.

[16] P. P. Vaidyanathan, *Multirate Systems and Filter Banks*. Englewood Cliffs, NJ: Prentice-Hall, 1993, pp. 859–863.

[17] I. H. Khoo, H. C. Reddy, L. D. Van, and C. T. Lin, "Generalized formulation of 2-D filter structures without global broadcast for VLSI implementation," presented at the IEEE MWSCAS, Seattle, WA, Aug. 2010

Pei-Yu Chen (S'10) was born in Taipei, Taiwan. She received the B.S. and M.S. degrees in engineering and system science from National Tsing Hua University (NTHU), Hsinchu, Taiwan, in 2004 and 2007, respectively. She is currently working toward the Ph.D. degree with the Department of Computer Science, National Chiao Tung University (NCTU), Hsinchu. Her research interests include digital signal processing and VLSI design.

Lan-Da Van (S'98-M'02) received the B.S. (Honors) and M.S. degrees from Tatung Institute of Technology, Taipei, Taiwan, in 1995 and 1997, respectively, and the Ph. D. degree from National Taiwan University (NTU), Taipei, in 2001, all in electrical engineering.

From 2001 to 2006, he was an Associate Researcher at National Chip Implementation Center (CIC), Hsinchu, Taiwan. In February 2006, he joined the faculty of the Department of Computer Science, National Chiao Tung University, Hsinchu, where he is currently an Assistant Professor. His research interests are in VLSI algorithms, architectures, and chips for digital signal processing and 3-D graphics systems. This includes the design of high-performance/low-power/cost-effective 3-D graphics systems, computer arithmetic, adaptive filters, transform, and platform-based system-on-a-chip (SOC) designs. He has published more than 40 journal and conference papers and holds one U.S. and one Taiwan patens in these areas.

Dr. Van was a recipient of the Chunghwa Picture Tube (CPT) and Motorola fellowships in 1996 and 1997, respectively. He was an elected chairman of the IEEE NTU Student Branch in 2000. In 2002, he received the IEEE award for outstanding leadership and service to the IEEE NTU Student Branch. In 2005, he was a recipient of the Best Poster Award at iNEER Conference for Engineering Education and Research (iCEER). Since 2009, he has served as the officer of the IEEE Taipei Section. He has served as a reviewer for several IEEE Transactions.

I-Hung Khoo (M'03) received the Ph.D. degree in electrical and computer engineering from the University of California, Irvine, in 2002.

He was a Senior IC Design Engineer at Agilent/Avago Technologies. He joined the Department of Electrical Engineering at California State University, Long Beach, as an Assistant Professor in 2006. His research interests include high-speed circuit design and analog and digital signal processing.

Dr. Khoo is currently serving as an officer of the IEEE Systems Council Chapter in the Coastal Los Angeles Section.

Haranatha (Hari) C. Reddy (M'77-SM'82-F'92) received the B.E. degree in electrical engineering from Sri Venkateswara University, Tirupati, India, the M.E. degree in electrical engineering from M.S. University of Baroda, Baroda, India, and the Ph.D. degree in ECE, from Osmania University, Hyderabad, India.

He has been with the Department of Electrical Engineering, California State University, Long Beach, as a tenured Full Professor since 1987. He was with the EE Department at Tennessee Technological University, Cookeville, Tennessee as an Associate Professor/Professor from 1980-87. Before joining Tennessee Tech, Dr. Reddy held teaching and research positions at the State University of New York College at Buffalo; Concordia University, Montreal, Canada; Osmania University, Hyderabad, India; and S.G.S. Institute of Science and Technology, Indore, India. Professor Reddy was appointed in 2007 as Chair Professor at National Chiao Tung University (NCTU) in Taiwan where he is also serving as Founding Director of the Center for Circuit Theory, Communications and Signal Processing. From 1993-99 he was a Guest Professor at the Institutes for Signal and Information Processing, and Integrated Systems, Swiss Federal Institute of Technology (ETH), Zurich, Switzerland; and as Visiting Researcher from 1994 to 1999 in the Department of Electrical and Computer Engineering at the University of California, Irvine. In 2003, he was awarded Honorary Professorship of the Technical University of Iasi, Iasi, Romania. His teaching and research interests are in the broad areas of circuit design, filters, systems, and signal processing. His research is concerned with the theory and applications of multidimensional circuits, systems, and digital filters. He has also been working on the development of filter theory for high-speed signal processing and other related problems using delta discrete time operator. He has coauthored about 140 research papers in journals/conferences and four book chapters. He attended and presented papers in over 50 IEEE international conferences.

Dr. Reddy was a Guest Editor for the special issue "Research and Education: Circuits and Systems" of the IEEE TRANSACTIONS ON EDUCATION published in August 1989. He served as the Principal Associate Editor for the IEEE TRANSACTIONS ON EDUCATION from 1984 to 1990. From 1993 to 1996, he was also an Associate Editor for IEEE TRANSACTIONS ON CIRCUITS AND SYSTEMS—PART I: FUNDAMENTAL THEORY AND APPLICATIONS and also served as an Associate Editor for the *Journal of Circuits, Systems and Computers*. In 1999, he co-organized and served as General Chair of the IEEE Circuits and Systems Society (CASS) 3rd Emerging Technologies Workshop on Mixed Signal Integrated Circuit Design (MSICD) held in Long Beach, CA. He served as the President-elect, President, and past President of the IEEE CASS in 2000, 2001, and 2002, respectively. Earlier, he served as CASS Vice President for Conferences for three years (1996, 1997, and 1999). From 1993 to 1995, he was a member of the IEEE CASS Board of Governors. He has served as Chair of the IEEE CASS Fellows Evaluation Committee in 2003 and 2004. He is a recipient of the 2003 IEEE CASS Meritorious Service Award. In 2003, he also received the diploma of honorary member of the Senate of the Technical University of Iasi, Romania, and the "Gh. Asachi" University Medal for outstanding contributions in the activities of cooperation with the faculties of the Technical University. He is a recipient of the Distinguished Faculty Scholarly and Creative Achievement Award (1990) and the Outstanding Professor Award (1993) from the California State University at Long Beach. He has also received in 1990 and 1992 the TRW Excellence in Research and Teaching Awards.

Dr. Chin-Teng (CT) Lin (S'88-M'91-SM'99-F'05) received the B.S. degree in control engineering from National Chiao-Tung University (NCTU), Hsinchu, Taiwan, in 1986 and the M.S.E.E. and Ph.D. degrees in electrical engineering from Purdue University, West Lafayette, IN, in 1989 and 1992, respectively.

Since August 1992, he has been with the College of Electrical Engineering and Computer Science, NCTU, where he is currently the University Provost and the Chair Professor of Electrical and Control Engineering. He served as the Founding Dean of Computer Science College of NCTU from 2005 to 2007. He is the textbook author of *Neural Fuzzy Systems* (Prentice-Hall) and *Neural Fuzzy Control Systems with Structure and Parameter Learning* (World Scientific). He has published over 140 journal papers, including about 80 IEEE Transactions papers. His research interests are in intelligent technology, soft computing, brain–computer interface, smart living technology, intelligent transportation systems, robotics and intelligent sensing, and nanobioinformation technologies and cognitive science (NBIC).

Dr. Lin is a member of Tau Beta Pi, Eta Kappa Nu, and Phi Kappa Phi honorary societies. He was a member of the Board of Governors (BoG) of the IEEE Systems, Man, Cybernetics Society (SMCS) from 2003 to 2005 and IEEE Circuit and Systems Society (CASS) (2005-2008), and the current BoG member of IEEE Computational Intelligence Society (CIS) (2008–2010). Dr. Lin is the IEEE Distinguished Lecturer from 2003 to 2005. He served as the Deputy EIC of the IEEE TRANSACTIONS OF CIRCUITS AND SYSTEMS—PART II, EXPRESS BRIEFS (2007–2008). Dr. Lin is the General Chair of FUZZ-IEEE2011 to be held in Taipei, and was the Program Chair of the 2006 IEEE International Conference on Systems, Man, and Cybernetics held in Taipei. He was the president of Board of Government (BoG) of Asia Pacific Neural Networks Assembly (APNNA) from 2004 to 2005. He has won the Outstanding Research Award granted by National Science Council (NSC), Taiwan, from 1997 to the present, the Outstanding Professor Award granted by the Chinese Institute of Engineering (CIE) in 2000, and the 2002 Taiwan Outstanding Information-Technology Expert Award. He was also elected to be one of 38th Ten Outstanding Rising Stars in Taiwan (2000).